Archives of Materials Science and Engineering

Volume 123
Issue 2
October 2023
Pages 72-85

International Scientific Journal
published monthly by the
World Academy of Materials
and Manufacturing Engineering

DOI: 10.5604/01.3001.0054.2494

Effect of artificial ageing temperature in T6-heat treatment on the mechanical properties of dissimilar metals weld between AA5083 and AA6063

H. Setyawan [a], N. Muhayat [a], M.Z. Yuliadi [b], Y.H.P. Manurung [c], Triyono [a,*]

[a] Mechanical Engineering Department, Sebelas Maret University (UNS), Surakarta, Indonesia
[b] Mechanical Engineering Department, Muhammadiyah University Surabaya, Surabaya, Indonesia
[c] School of Mechanical Engineering, University of Technology Mara (UiTM), 40450 Shah Alam, Selangor, Malaysia
* Corresponding e-mail address: triyono74@staff.uns.ac.id
ORCID identifier: https://orcid.org/0000-0003-4562-0628 (T.)

ABSTRACT

Purpose: Aluminium AA5083 is commonly utilised in constructing ship hull shells, which are welded with aluminium AA6063 to act as stiffeners. However, the joints often suffer structural damage, such as longitudinal and transverse cracks in the dissimilar weld area, particularly in the Heat-Affected Zone (HAZ) of AA6063, which includes frames, brackets, and collars. To enhance the mechanical properties of AA6063, T6 heat treatment is commonly employed. The given study investigates the impact of temperature in artificial ageing during the T6 heat treatment on the microstructure and mechanical properties of the dissimilar materials welding between AA5083 and AA6063.

Design/methodology/approach: The T6 heat treatment variations involve a solution treatment at 540°C for 6 hours, followed by quenching and artificial ageing at temperatures of 158°C, 200°C, and 230°C for 6 hours, followed by air cooling. The T6 heat treatment variations involve a solution treatment at 540°C for 6 hours, followed by quenching and artificial ageing at temperatures of 158°C, 200°C, and 230°C for 6 hours, followed by air. The weld joints were visually inspected and examined using radiography, then characterised by microstructure investigation and tensile and impact tests.

Findings: The study's findings reveal that the T6 heat treatment significantly improves the mechanical properties of AA6063. However, the T6 heat treatment does not notably affect the mechanical properties of AA5083, the fusion line and the weld metal area. Among the artificial ageing temperature variations, the highest mechanical properties are achieved at 200°C, while the lowest mechanical properties are observed at 230°C.

Research limitations/implications: Aluminium AA5083 is commonly utilised in constructing ship hull shells, which are welded with aluminium AA6063 to act as stiffeners. However, the joints often suffer structural damage, such as longitudinal and transverse cracks in the dissimilar weld area, particularly in the Heat-Affected Zone (HAZ) of AA6063, which includes frames, brackets, and collars. The paper focused on the influence of artificial ageing temperature in T6 heat treatment on the microstructure and mechanical properties of the dissimilar metals welding between AA5083 and AA6063.

Originality/value: The optimum artificial ageing temperature in T6 heat treatment for the dissimilar metals welding between AA5083 and AA6063 was 200°C. The method can be applied in ship structures where AA5083 is typically utilised for constructing the hull shells, while AA6063 is employed as stiffeners.

Keywords: Dissimilar metals weld, AA6063, AA5083, Artificial ageing temperature, T6 heat treatment

Reference to this paper should be given in the following way:

H. Setyawan, N. Muhayat, M.Z. Yuliadi, Y.H.P. Manurung, Triyono, Effect of artificial ageing temperature in T6-heat treatment on the mechanical properties of dissimilar metals weld between AA5083 and AA6063, Archives of Materials Science and Engineering 123/2 (2023) 72-85. DOI: https://doi.org/10.5604/01.3001.0054.2494

MATERIALS MANUFACTURING AND PROCESSING

1. Introduction

Aluminium is widely recognised as a versatile metal in various manufacturing industries due to its lightweight nature, white colour, distinctive shiny appearance, high corrosion resistance, good formability and weldability [1-8]. In ship construction, achieving lightweight, strong and corrosion resistance properties is crucial, and two commonly combined aluminium alloys for the purpose are AA5083 and AA6063 [9]. AA5083 is a non-heat-treatable and high corrosion-resistant aluminium alloy consisting primarily of aluminium and magnesium [1, 10-12]. On the other hand, AA6063 is a heat-treatable and strong aluminium alloy that contains aluminium, magnesium, and silicon [13-17].

Within shipbuilding, AA5083 and other 5XXX series are typically utilised for constructing the hull shells, while AA6063 is employed as stiffeners [18-20]. However, welding AA5083 and AA6063 joints in ships often leads to structural damage, particularly in the heat-affected zone (HAZ) of AA6063. It can manifest as longitudinal and transverse cracks [17] caused by the heat input during the welding process [1,21,22]. The heat input alters the microstructure of the welded AA6063, resulting in the formation of precipitates, changes in grain size, the presence of geometrically necessary dislocations (GNDs), and the clustering of Mg_2Si precipitates at grain boundaries, especially in the HAZ of AA6063 [13,19,23]. Heat treatment is employed to address mechanical property degradation, particularly the T6 heat treatment, known for its effectiveness in enhancing the mechanical properties of heat-treatable aluminium alloys like AA6063 [13,19,24]. The T6 heat treatment involves a solution treatment followed by artificial ageing. It helps to restore precipitate formation, refine grain size, increase the number of GNDs, and achieve a uniform distribution of Mg_2Si precipitates [13,19, 24-27]. The choice of artificial ageing temperature within the T6 heat treatment range significantly impacts the resulting mechanical properties. The optimal artificial aging temperature for improving the mechanical properties of AA6063 typically falls between 150°C and 230°C [19].

If the dissimilar metals weld between AA5083 and AA6063, which naturally consists of non-heat-treatable and heat-treatable aluminium, undergoes T6 heat treatment, the response of each material will differ. T6 heat treatment will improve the microstructure and mechanical properties of AA6063. Still, it is unlikely to significantly affect the microstructure and mechanical properties of AA5083 since it is a non-heat-treatable aluminium [28]. The response to T6 heat treatment in the transitional region between the two metals is particularly interesting, with a non-heat-treatable to heat-treatable transition. Based on reference studies, the influence of T6 heat treatment, especially the artificial ageing temperature, on the mechanical properties in the transitional region of dissimilar metals weld between AA5083 and AA6063 has yet to be discussed. The research investigates the effect of artificial ageing temperature in T6 heat treatment on the mechanical properties of dissimilar metals weld between AA5083 and AA6063. The T6 heat treatment process involves a solution treatment at 540°C for 6 hours, followed by quenching using water, and subsequent artificial ageing at temperatures of 158°C, 200°C, and 230°C for 6 hours, with final air cooling.

2. Experimental methods

The AA5083 and AA6063 aluminium plates have 300 x 150 x 6 mm dimensions. The chemical composition of the base metal and welding wire can be seen in Table 1, while the mechanical properties of the base metal and welding wire can be seen in Table 2. The GMAW (Gas Metal Arc Welding) process used the Merkle compact MIG Pro 210K to weld the AA6063 and AA5083 aluminium. The welding parameters used in the process adhere to ASTM E30 standards.

Table 1.
The chemical composition of the base metal and welding wire.

Element	Si	Fe	Cu	Mn	Mg	Cr	Zn	Ti	Al
AA5083	0.32	0.29	0.44	0.88	4.73	0.09	0.22	0.02	Balance
AA6063	0.44	0.28	0.03	0.01	0.62	0.05	0.04	0.02	Balance
ER5356	0.25	0.4	0.1	0.05	4.5	0.05	0.1	0.06	Balance

Table 2.
The mechanical properties of the base metal and welding wire

Materials	Tensile strength, MPa	Elongation,%
AA5083	346	27
AA6063	204	11
ER5356	240	17

The groove and root dimensions of the welding joint can be seen in Figure 1. The GMAW process utilised a 1.2 mm diameter ER5356 welding wire, a wire speed of 5.5 m/min, a welding speed of 20.7 cm/min, a voltage of 22 V, and a current of 170 A. Argon 99% shielding gas was used with a flow rate of 18 l/min. The results of the GMAW process can be observed in Figure 2.

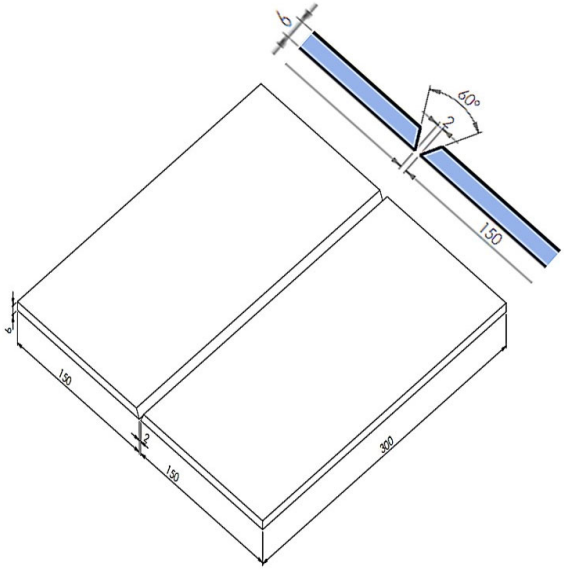

Fig. 1. Test coupon for weld joint

After the welding process was completed, the weld joints were visually inspected and examined using radiography. Radiographic testing is employed to detect defects within the material without damaging it by utilising X-rays or gamma rays [29-31]. If it was confirmed that there were no defects, then the T6 heat treatment process was conducted on the welded specimens with heat treatment parameters, as presented in Table 3. The T6A, T6B, and T6C heat treatment diagrams can be seen in Figure 3. The B-One ceramic fibre muffle furnace 2020 model FNC-7 was used for the heat treatment. Subsequently, the specimens were cut to obtain the required dimensions according to the standard test specimen.

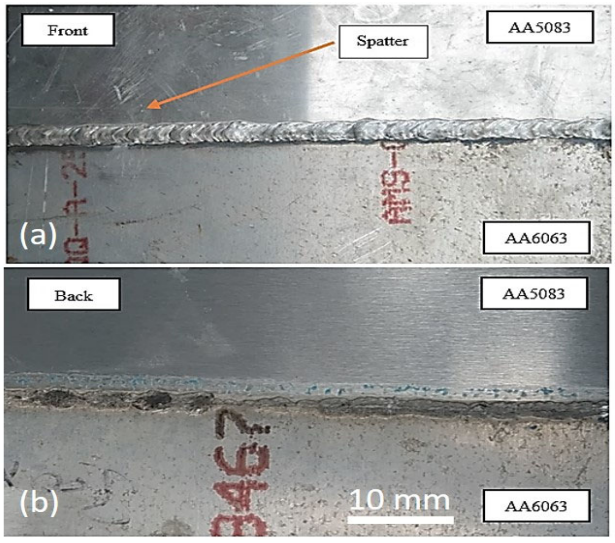

Fig. 2. Bead appearance of dissimilar metals weld between AA5083 and AA6063 (a) welded face, (b) back face

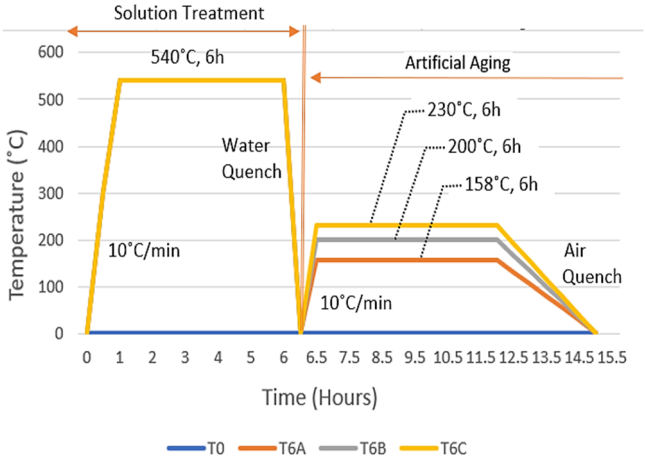

Fig. 3. Heat treatment diagram

Table 3.
The research parameters

No	Code	Heat treatment T6	
		Solution treatment	Artificial aging
1	T0	Without	Without
2	T6A	540°C holding time 6 hours	Temperature 158°C holding time 6 hours
3	T6B	540°C holding time 6 hours	Temperature 200°C holding time 6 hours
4	T6C	540°C holding time 6 hours	Temperature 230°C holding time 6 hours

Macrostructure testing was conducted using the Olympus stereo zoom microscope model SZ2-ILTS, while microstructure testing was performed using the Euromex Holland optical microscope model iScope IS.1153-PLi. The specimens to be tested for both microstructure and macrostructure were prepared by grinding with sandpaper up to 2200 grit. The etching process was carried out using Keller's reagent, which consisted of 5 ml of nitric acid, 3 ml of hydrochloric acid, 2 ml of hydrofluoric acid, and 190 ml of distilled water. Hardness testing was also performed on the specimens using micro Vickers Highwood HWMMT X7 with a load of 100 g. Microstructure and hardness were tested on the parent metal, heat-affected zone (HAZ), fusion line, and weld metal. The dimensions of the macrostructure, microstructure, and hardness test specimens can be seen in Figure 4.

Tensile testing was performed to determine tensile strength, yield strength, and elongation using the Sans Universal Testing Machine model SHT-4106. The tensile test specimens were prepared according to the AWS D.1.2 standard, as shown in Figure 5. The fractured tensile test specimens were observed using a stereo-zoom microscope to identify the type and mechanism of material fracture.

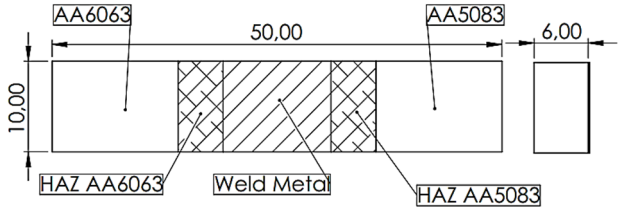

Fig. 4. The dimensions of the macrostructure, microstructure, and hardness test specimens

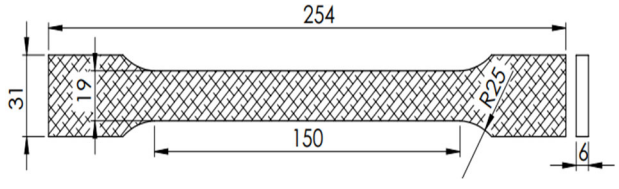

Fig. 5. The dimensions of the tensile test specimen

Impact testing was performed using the Tatonas Charpy impact machine with a capacity of 300 joules. According to the ISO 9016 standard, the impact testing of the weld joint was conducted at 7 points: on the AA5083 base metal, AA5083 HAZ, AA6063 base metal, AA6063 HAZ, AA6063 fusion line, AA5083 fusion line, and weld metal. The impact test specimens, in accordance with the ISO 9016 standard, are illustrated in Figure 6. The fractured test specimens were observed using a stereo-zoom microscope to identify the type and mechanism of material fracture due to impact load.

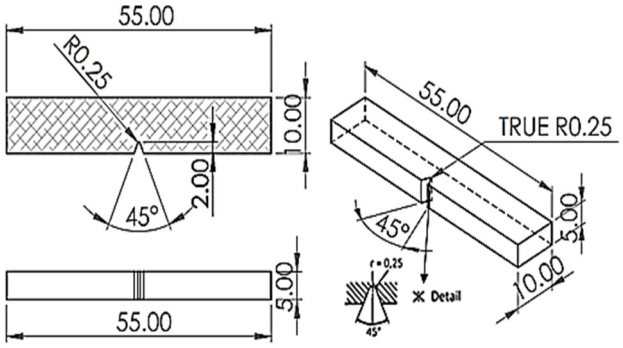

Fig. 6. The dimensions of the impact test specimen

3. Results obtained

3.1. Result of radiographic test

Certified welders performed the welding process; however, defects were still present in the weld, specifically porosity and incomplete penetration. The issues are evident in the radiographic testing results depicted in Figure 7.

Fig. 7. Radiographical image of the weld joint

3.2. Result of macrostructure investigation

Further confirmation of the radiographic test results can be obtained through the observation of the macrostructure of the welding results, as presented in Figure 8a. Consistent with the radiographic tests, the welded joint exhibits defects in the form of porosity and incomplete penetration. Porosity defects in aluminium welding are commonly caused by the extreme difference in hydrogen gas solubility between liquid and solid aluminium. During solidification, hydrogen gas becomes trapped due to the rapid cooling, forming pores within the weld [32-34]. In the case of incomplete penetration in aluminium welding, it can be attributed to the high thermal conductivity of aluminium. The high thermal conductivity of aluminium causes the welding heat workpiece to spread throughout the entire workpiece rapidly. Consequently, the heat to melt the aluminium is reduced, leading to insufficient penetration in the weld [35].

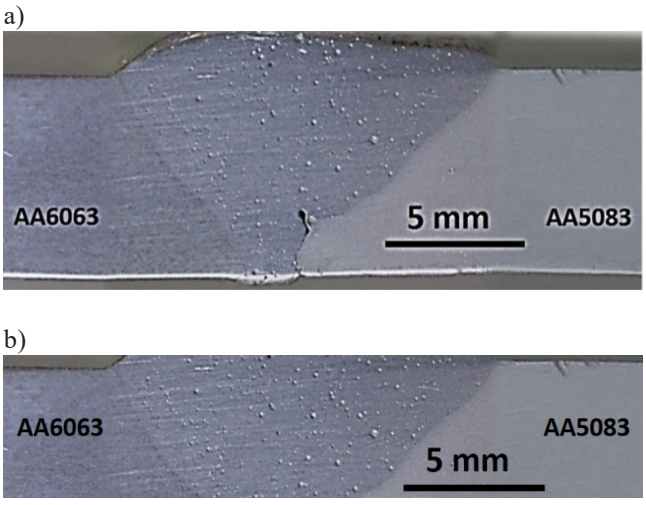

Fig. 8. Macrostructure of the weld joint: a) before cutting, b) after cutting for removing geometrical defects

The presence of geometric defects, such as incomplete penetration, can significantly impact the properties of the welded joint and disrupt the intended effects of the predetermined research parameters. To mitigate the impact of incomplete penetration, the root portion of the weld joint was removed using a milling process, as depicted in Figure 8(b). However, it is important to note that porosity defects could not be eliminated during the study. It was assumed that all specimens exhibited the same porosity defect, attributing any changes in the properties of the weld joint solely to the effects of the T6 heat treatment.

3.3. Result of microstructure investigation

The microstructure of the base metal region of AA5083 is depicted in Figure 9. Heat treatment induces changes in grain size, which initially consists of small and elongated grains. However, the grain size increases after heat treatment, specifically T6A, T6B, and T6C. Figure 10 illustrates the microstructure of the weld metal region before and after T6 heat treatment. The grain size remains unchanged before and after heat treatment, including TGA, T6B, and T6C.

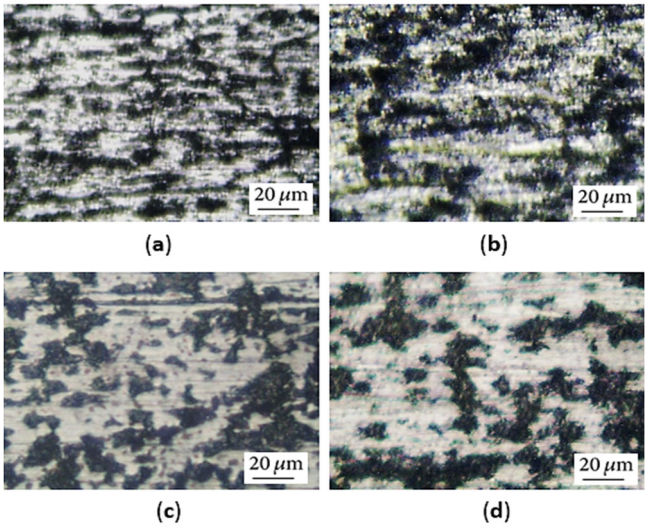

Fig. 9. Microstructure of base metal AA5083: (a) T0; (b) T6A; (c) T6B; (d) T6C

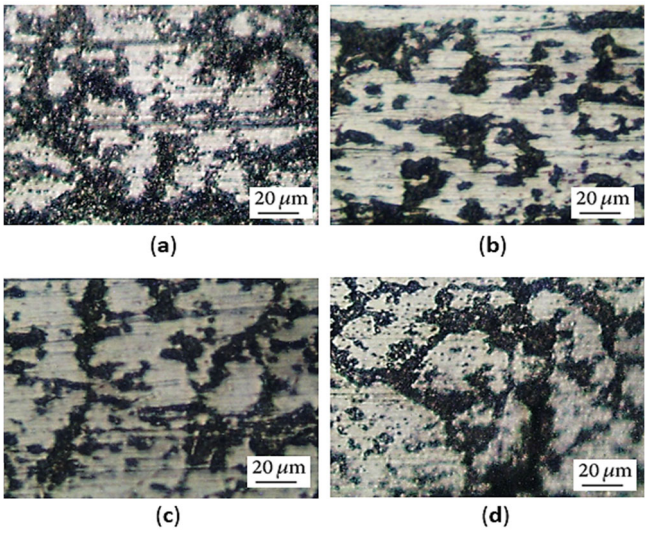

Fig. 10. Microstructure of weld metal: (a) T0; (b) T6A; (c) T6B; (d) T6C

Regarding the parent metal, AA6063, its microstructure is presented in Figure 11. The grain size undergoes modifications, transitioning from relatively large and non-uniform grains. Following heat treatment, both T6A and T6B, the grain size becomes smaller and tends to exhibit more uniformity. Surprisingly, heat treatment T6C results in an increase in grain size. The microstructure within the transition region between AA6063 and the weld metal is illustrated in Figure 12. Figure 12a showcases an untreated specimen, where the Mg_2Si precipitates are relatively large, clustered, and non-uniform. Figure 12b demonstrates that after undergoing T6A heat treatment, the size of Mg_2Si precipitates in the AA6063 region decreases, dispersing within the α Al-Mg-Si matrix. However, the size of the precipitates tends to be non-uniform and larger than those in the T6B specimen. Figure 12c reveals that after T6B heat treatment, the Mg_2Si precipitates in the AA6063 region become the smallest among the examined specimens. Finally, Figure 12d indicates that after T6C heat treatment, the Mg_2Si precipitates tend to dissolve within the α Al-Mg-Si matrix and accumulate at the grain boundaries.

3.4. Result of hardness test

The hardness distribution in the vicinity of the weld joint is illustrated in Figure 13. According to the image, the base metal and Heat-Affected Zone (HAZ) of AA5083 tend to exhibit a slight decrease in hardness after undergoing heat

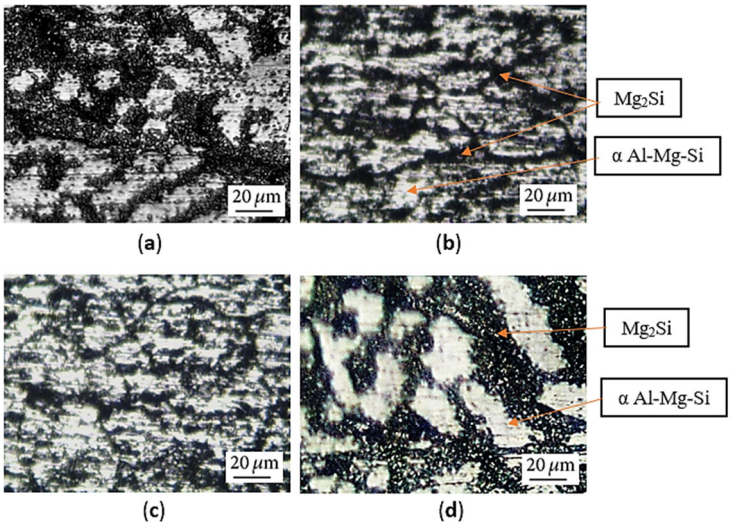

Fig. 11. Microstructure of base metal AA6063: (a) T0; (b) T6A; (c) T6B; (d) T6C

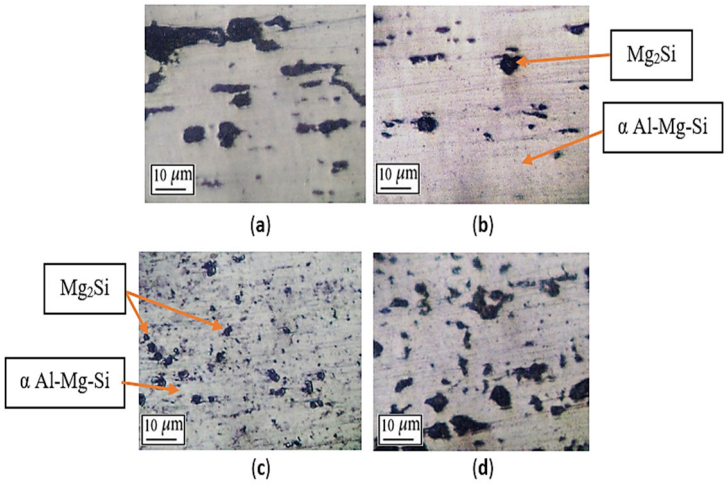

Fig. 12. Microstructure of AA6063-weld metal transition: (a) T0; (b) T6A; (c) T6B; (d) T6C

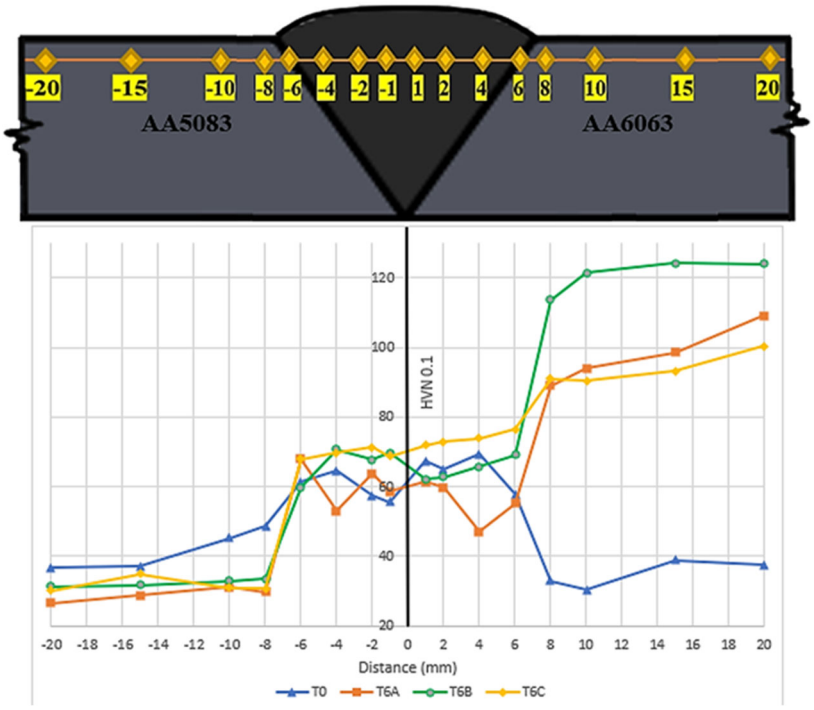

Fig. 13. Hardness distribution of dissimilar metals weld

treatment, including T6A, T6B, and T6C. Conversely, the weld metal region demonstrates relatively consistent hardness across T0, T6A, T6B, and T6C. It suggests that the T6 heat treatment process has a limited impact on the hardness of the weld metal. In contrast, both the HAZ and base metal of AA6063 demonstrate an increase in hardness after undergoing heat treatment, including T6A, T6B, and T6C. Notably, T6B exhibits the highest increase in hardness among the treatments for both the HAZ and base metal of AA6063.

3.5. Result of tensile test

Tensile tests in dissimilar metals weld joints which experienced heat treatment T6 with various levels of artificial ageing temperature are presented in Figure 14. The figure indicates that the tensile strength of the dissimilar metal weld joint between AA5083 and AA6061 generally increases after undergoing the T6 heat treatment process, regardless of the artificial ageing temperature (158°C, 200°C, or 230°C). The untreated dissimilar metal weld joint exhibits a tensile strength of approximately 98 MPa, and the fracture surface and shape are seen in Figure 15. In contrast, the T6 heat-treated weld joint demonstrates a tensile strength exceeding 200 MPa. However, the increase in tensile strength is accompanied by a decrease in the weld joint's ductility, as evidenced by reduced elongation and changes in the fracture surface and shape (Figs. 16-18). Among the three levels of artificial ageing temperature, the T6 heat treatment with an artificial ageing temperature of 200°C (specimen T6B) is considered the optimal condition. Specimen T6B exhibits the highest tensile strength, with a relatively minor reduction in ductility compared to the untreated specimen. The fracture section reveals the presence of necking and a rough fracture surface (Fig. 17). In contrast, specimen T6C, subjected to the T6 heat treatment with an artificial ageing temperature of 230°C, displays the lowest tensile strength and ductility among the specimens with T6 heat treatment. The tensile fracture does not exhibit necking, and the fracture surface is flat and bright, indicating a brittle fracture (Fig. 18).

3.6. Result of impact test

The impact test results of dissimilar metal weld specimens AA5083-AA6061, which underwent T6 heat treatment with various artificial ageing temperatures, are presented in Figure 19. The notches in the impact test specimens were strategically placed in the Heat-Affected Zone (HAZ), fusion line, and weld metal. Notably, aluminium AA5083 and AA6061 demonstrate distinct responses to T6 heat treatment. In the parent metal and HAZ

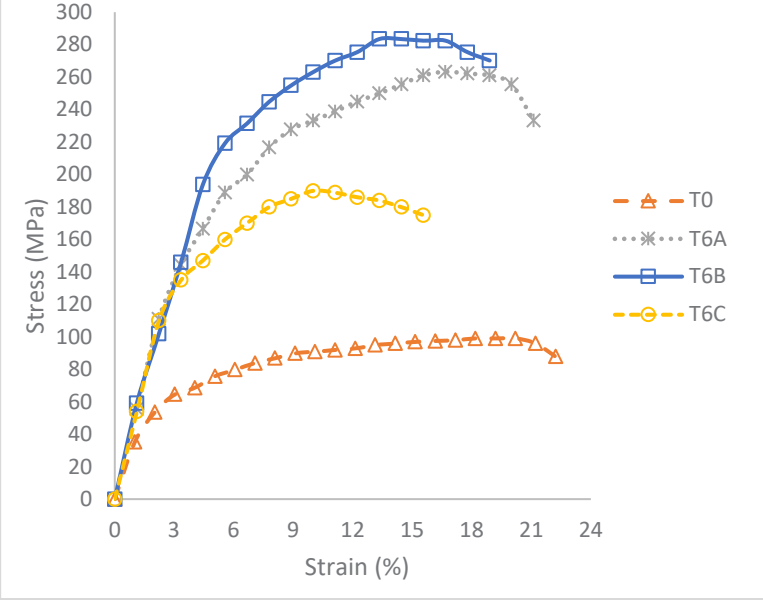

Fig. 14. Stress-strain diagram of dissimilar metals weld

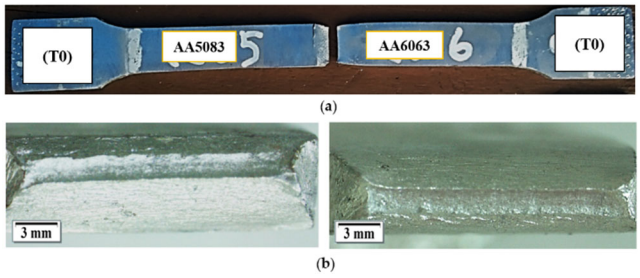

Fig. 15. a) Fractured specimen T0; b) Macrostructure of the fracture surface of T0

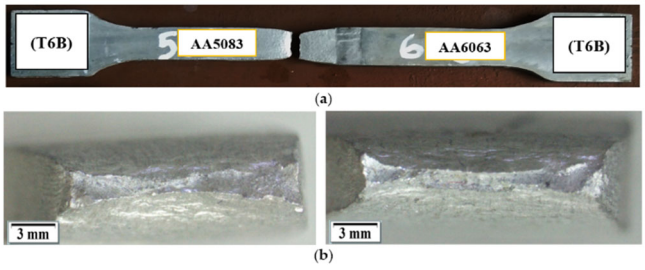

Fig. 17. a) Fractured specimen T6B; b) Macrostructure of the fracture surface of T6B

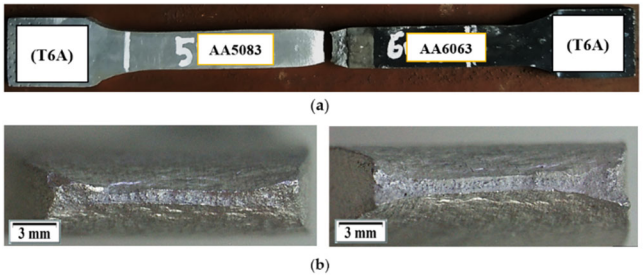

Fig. 16. a) Fractured specimen T6A; b) Macrostructure of The fracture surface of T6A

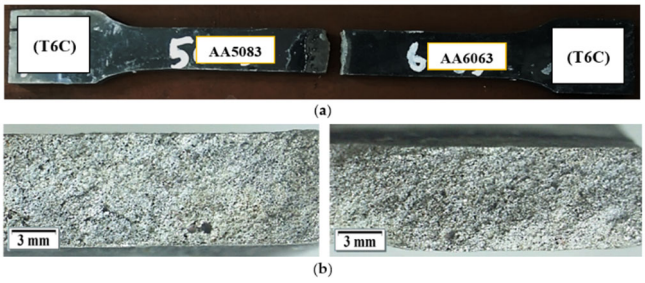

Fig. 18. a) Fractured specimen T6C; b) Macrostructure of the fracture surface of T6C

of AA5083, T6 heat treatment reduces the impact strength, whereas in the parent metal and HAZ of AA6061, T6 heat treatment enhances the impact strength. The T6 heat treatment also results in a slight improvement in the impact strength of the weld metal. It is attributed to the relatively large, clustered, and non-uniform Mg_2Si precipitates. As depicted in Figure 20a, the surface fracture of the untreated specimen appears coarse.

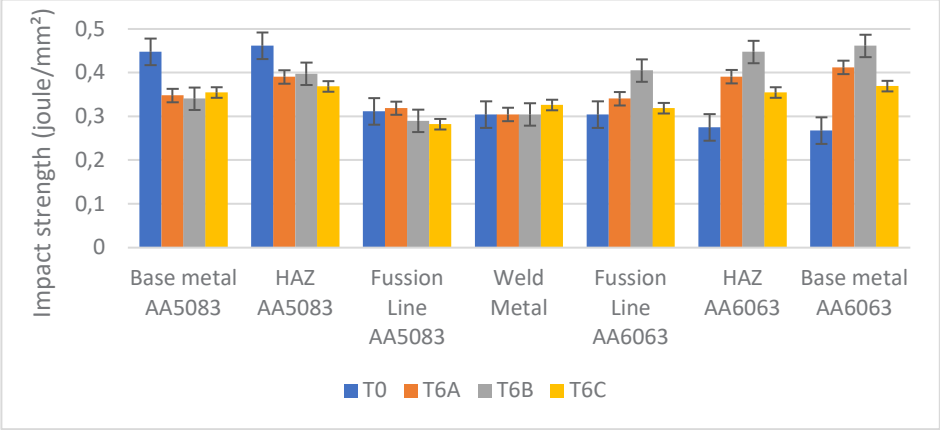

Fig. 19. Impact strength of specific zone in dissimilar metals weld joint

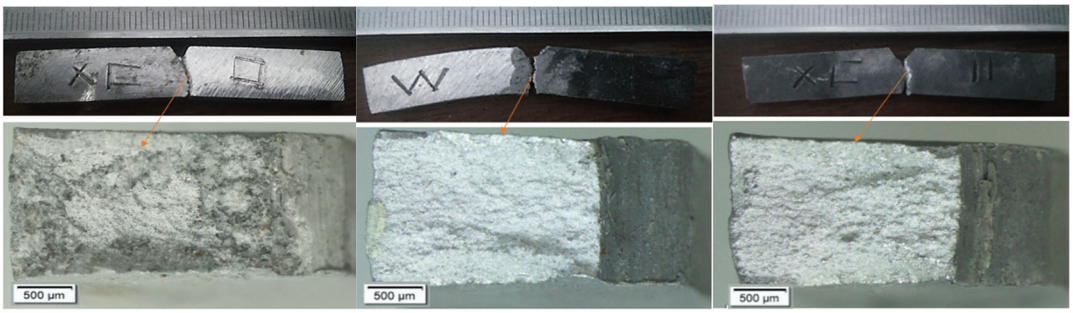

(a) (b) (c)

Fig. 20. Surface fracture of impact test specimen with the notch in weld metal: a) T0, b) T6B, c) T6C

Conversely, Figures 20b and c show that the surface fracture of T6B and T6C is much finer. The findings align with the observations of microstructure and hardness distribution. Interestingly, the fusion line of AA5083, weld metal, and fusion line of AA6061 exhibit relatively similar impact strength. Consequently, it can be concluded that the T6 heat treatment process has minimal influence on the impact strength in the transition region and weld metal.

4. Discussion

After undergoing T6 heat treatment, the base metal AA5083 shows a slight decrease in hardness and impact strength, although the decrease is insignificant. The reduction in hardness and impact strength is primarily attributed to the change in grain size of the AA5083 base metal rather than a phase change. AA5083 aluminium is classified as a non-heat-treatable material and should not undergo significant changes in hardness during heat treatment. However, in the given study, the observed decrease in hardness of the base metal AA5083 can be attributed to the prior strain hardening of the aluminium through H112 rolling during its production, which is subsequently nullified by the heat treatment process. The strain-hardened AA5083 aluminium exhibits smaller elongated grain sizes due to the rolling process, as depicted in Figure 9a. The characteristic generally leads to improved mechanical properties, including increased hardness. Nevertheless, the heat treatment process induces recrystallisation in the base metal AA5083-H112, causing the elimination of the strain hardening effect resulting from H112 rolling. Consequently, the grain size returns to a normal or even larger state, as observed in Figures 9b, 9c, and 9d [26].

The analysis of impact strength and the corresponding fractures observed on the surface of the fractured impact test specimens provide valuable insights into the mechanical properties of the material. Intergranular and transgranular fractures in untreated specimens (T0) suggest that the material is more susceptible to brittle fractures, where cracks propagate along grain boundaries and cause the material to fail without significant plastic deformation. Research by Wang et al. [36] highlights the correlation between

intergranular fractures and low-impact strength, as well as the connection between ductile fractures and higher mechanical properties. On the other hand, specimens T6A and T6B, which exhibit moderate and high impact strength, respectively, display ductile fractures on their surfaces. Ductile fractures are characterised by plastic deformation before final failure, allowing the material to absorb more energy and exhibit higher impact strength. The plastic deformation in the specimens helps prevent sudden and catastrophic failure, improving mechanical properties [36,37].

The analysis of the transition zone of AA5083 and the weld metal after T6 heat treatment revealed no significant changes in hardness and impact strength. The observation aligns with the findings of a study conducted by Verma et al. [38], which investigated the microstructural and mechanical properties of AA5083 welds subjected to heat treatment. The lack of influence on material hardness after T6 heat treatment could be attributed to the grain size in the transition zone of AA5083 and the weld metal. They found that the grain size in the weld metal region, including T0, T6A, T6B, and T6C, remained relatively similar, as evidenced by their microstructural analysis in Figure 10. The minimal change in grain size despite T6 heat treatment can be attributed to the specific welding process employed. The Gas Metal Arc Welding (GMAW) process used to join AA5083 and AA6063, using ER 5356 filler material, is well-known for its capability to produce welds with fine and uniform grain structures. As ER 5356 is classified as a non-heat-treatable filler material, the subsequent T6 heat treatment had little impact on the grain size of the weld metal region. The findings support the results of previous research by Verma et al. on the influence of welding processes and filler materials on the microstructure and mechanical properties of welded alloys [38-40]. They emphasised that selecting appropriate filler materials, especially non-heat-treatable ones, can result in stable microstructures even after heat treatments.

The transition region and base metal AA6063 experienced a significant increase in hardness and impact strength after T6 heat treatment. The enhancement can be attributed to two key factors: changes in grain size and the dispersion of β-phase Mg_2Si precipitates within AA6063 [13,23,41]. Mg_2Si, an aluminium 6xxx precipitate, is observed as dark particles scattered throughout the aluminium matrix. The intermetallic compound has a face-centred cubic (FCC) crystal lattice structure with a lattice parameter (a) of 6.351 Å. Its composition comprises 63.2% Mg atom and 38.8% Si atom [13]. In the untreated AA6063 transition region (T0), the microstructure reveals relatively large and non-uniform grain sizes, accompanied by agglomerated Mg_2Si precipitates at grain boundaries, as shown in Figure 11a and Figure 12a. The factors contribute to the lowest hardness and impact strength observed in the region.

On the other hand, the AA6063 transition region subjected to T6 heat treatment at an artificial ageing temperature of 158°C (specimen T6A) displays relatively smaller grain sizes than the untreated region (T0). However, the grain shape remains non-uniform. Mg_2Si precipitates begin to disperse throughout the microstructure, although some clustering at grain boundaries is still evident, as depicted in Figure 11b and Figure 12b. The presence of finer grain sizes and the more uniform distribution of Mg_2Si precipitates within the microstructure of the T6 heat-treated at an artificial ageing temperature of 158°C (specimen T6A) contribute to the significant increase in hardness and impact strength. The factors play a crucial role in enhancing the mechanical properties of aluminium [42]. The microstructure analysis of the AA6063 transition region subjected to T6 heat treatment at an artificial ageing temperature of 200°C (specimen T6B) reveals the presence of relatively small and uniform grain sizes, accompanied by a uniform dispersion of Mg_2Si precipitates throughout the matrix. The minimal occurrence of visible Mg_2Si clusters at grain boundaries, as observed in Figure 11c and Figure 12c, contributes to the exceptional hardness and impact strength exhibited by the AA6063 transition region of specimen T6B. However, with an increase in artificial ageing temperature to 230°C (specimen T6C), the microstructure of the AA6063 transition region undergoes a grain coarsening process, leading to non-uniform grain sizes. In addition, Mg_2Si precipitates tend to recluster at grain boundaries, as depicted in Figures 11d and 12d. The phenomenon is attributed to the over-aging effect experienced by AA6063 during the T6C heat treatment [24,26,27]. Consequently, the AA6063 T6C exhibits reduced hardness and impact strength, approaching values similar to those of untreated specimens (T0). The grain size and distribution of Mg_2Si precipitates play a crucial role in determining the hardness and impact strength of aluminium.

The T6 heat treatment in dissimilar metal welding between AA5083 and AA6063 significantly influences tensile strength. Specimens that did not undergo any treatment (T0) show low tensile strength, primarily due to the weakening of the material in the AA6063 transition region post-Gas Metal Arc Welding (GMAW). The weakening is largely attributed to the clustering of Mg_2Si precipitates at grain boundaries, as corroborated by Yürük et al. [1]. The phenomenon is visually evident in Figure 15, showcasing the fracture surface of the T0 tensile test specimens in the AA6063 transition region. However, a rise in tensile strength is observed after implementing T6 heat

treatment with artificial ageing temperatures of 150°C (T6A) and 200°C (T6B). The increase can be attributed to the considerable enhancement of AA6063's mechanical properties due to grain refinement and the even dispersion of Mg_2Si precipitates throughout the aluminium matrix [13,43,44]. The correlation between T6 heat treatment and an improvement in mechanical properties is reinforced by studies [38,39].

Moreover, the tensile fracture locations of the T6A and T6B specimens found within the AA5083 region, as shown in Figure 16 and Figure 17, further support the argument. Contrarily, T6C specimens (undergoing T6 heat treatment with an artificial ageing temperature of 230°C) experience reduced strength and ductility. It can be attributed to the material undergoing over-aging post T6C treatment, leading to a re-clustering of Mg_2Si precipitates at grain boundaries in the AA6063 transition region, as illustrated in Figure 11d and Figure 12d. The observation aligns with the fracture location of the T6C specimen, which reoccurs within the AA6063 transition region, as evident in Figure 18. In essence, the ageing of AA60xx aluminium alloys results in a deterioration of their mechanical properties [32,34,38, 43,45], serving as a compelling argument against such heat treatment practices. The findings highlight the importance of optimising artificial ageing temperature in the T6 heat treatment process to achieve desirable mechanical properties while avoiding procedures that can potentially diminish the attributes.

5. Conclusions

A study investigated the influence of artificial ageing temperature in T6 heat treatment on the mechanical properties of dissimilar metal welds, specifically AA5083 and AA6063. The following conclusions were drawn from the study:

- The artificial ageing temperature in T6 heat treatment significantly impacts improving the mechanical properties of the fusion zone and base metal of AA6063. It is achieved by evenly dispersing the β phase precipitates, Mg_2Si, within the α matrix of Al-Mg-Si.
- However, the artificial ageing temperature in T6 heat treatment does not significantly affect the changes in mechanical properties of the weld metal, HAZ AA5083, and base metal AA5083, as the materials are non-heat treatable.
- Among the various artificial ageing temperatures tested, 200°C was found to yield the best mechanical properties, while 230°C resulted in the worst mechanical properties.

Acknowledgements

The authors would like to thank Universitas Sebelas Maret Surakarta and DIKTI, Indonesia, for providing many facilities and financial support through the schema PTM grant 2023.

References

[1] A. Yürük, B. Çevik, N. Kahraman, Analysis of mechanical and microstructural properties of gas metal arc welded dissimilar aluminum alloys (AA5754/ AA6013), Materials Chemistry and Physics 273 (2021) 125117. DOI: https://doi.org/10.1016/j.matchemphys.2021.125117

[2] H. Pratikno, Aging Treatment to Increase the Erosion-Corrosion Resistance of AA6063 Alloys for Marine Application, Procedia Earth and Planetary Science 14 (2015) 41-46. DOI: https://doi.org/10.1016/j.proeps.2015.07.083

[3] A. Vinoth Jebaraj, K.V.V. Aditya, T. Sampath Kumar, L. Ajaykumar, C.R. Deepak, Mechanical and corrosion behaviour of aluminum alloy 5083 and its weldment for marine applications, Materials Today: Proceedings 22/4 (2020) 1470-1478. DOI: https://doi.org/10.1016/j.matpr.2020.01.505

[4] J.S. de Andrade, M.R.S. Vieira, S.H. Oliveira, S.K. de Melo Santos, S.L. Urtiga Filho, Study of microbiologically induced corrosion of 5052 aluminum alloy by sulfate-reducing bacteria in seawater, Materials Chemistry and Physics 241 (2020) 122296. DOI: https://doi.org/10.1016/j.matchemphys.2019.122296

[5] E. Fracchia, F. Gobber, M. Rosso, About weldability and welding of Al alloys: case study and problem solving, Journal of Achievements in Materials and Manufacturing Engineering 85/2 (2017) 67-74. DOI: https://doi.org/10.5604/01.3001.0010.8036

[6] H. Mehdi, R.S. Mishra, Mechanical properties and microstructure studies in Friction Stir Welding (FSW) joints of dissimilar alloy – a review, Journal of Achievements in Materials and Manufacturing Engineering 77/1 (2016) 31-40. DOI: https://doi.org/10.5604/17348412.1229666

[7] A.A. Saleh, Joining of AA2014 and AA5059 dissimilar aluminium alloys by Friction Stir Welding, Journal of Achievements in Materials and Manufacturing Engineering 97/1 (2019) 15-20. DOI: https://doi.org/10.5604/01.3001.0013.7945

[8] E. Korkmaz, A. Gülsöz, C. Meran, Investigations on the joint properties of the friction welding of aluminium alloy tube to tube plate using an external tool, Journal of Achievements in Materials and Manufacturing Engineering 81/2 (2017) 70-75. DOI: https://doi.org/10.5604/01.3001.0010.2040

[9] Z. Huda, N.I. Taib, T. Zaharinie, Characterization of 2024-T3: An aerospace aluminum alloy, Materials Chemistry and Physics 113/2-3 (2009) 515-517. DOI: https://doi.org/10.1016/j.matchemphys.2008.09.050

[10] L. Huang, X. Hua, D. Wu, Z. Jiang, F. Li, H. Wang, S. Shi, Microstructural characterization of 5083 aluminum alloy thick plates welded with GMAW and twin wire GMAW processes, International Journal of Advanced Manufacturing Technology 93 (2017) 1809-1817. DOI: https://doi.org/10.1007/s00170-017-0480-1

[11] V. Manikandan, K. Mariselvam, R. Nekin Joshua, C. Ramesh, K. Arunprasath, Study on process parameters of Tungsten Inert gas welded aluminium alloy 5086 through mechanical characteristics, Materials Today: Proceedings 66/3 (2022) 683-689. DOI: https://doi.org/10.1016/j.matpr.2022.03.641

[12] B. Cevik, B. Gülenç, The effect of welding speed on mechanical and microstructural properties of 5754 Al ($AlMg_3$) alloy joined by laser welding, Materials Research Express 5/8 (2018) 086520. DOI: https://doi.org/10.1088/2053-1591/aad3b0

[13] J.A. Muñoz, A. Komissarov, M. Avalos, R.E. Bolmaro, Heat treatment effect on an AA6063 alloy, Materials Letters 277 (2020) 128338. DOI: https://doi.org/10.1016/j.matlet.2020.128338

[14] X. Meng, S. Yang, Y. Huang, J. Fang, J. Gu, Q. Xiong, C. Duan, Microstructure characterization and mechanism of fatigue crack propagation of 6082 aluminum alloy joints, Materials Chemistry and Physics 257 (2021) 123734. DOI: https://doi.org/10.1016/j.matchemphys.2020.123734

[15] M. Pakdil, G. Çam, M. Koçak, S. Erim, Microstructural and mechanical characterization of laser beam welded AA6056 Al-alloy, Materials Science and Engineering A 528/24 (2011) 7350-7356. DOI: https://doi.org/10.1016/j.msea.2011.06.010

[16] J. Liu, M.J. Tan, A.E.W. Jarfors, S.C.V. Lim, K.S. Fong, S. Castagne, Greener manufacturing: Superplastic-like forming, Journal of Physics: Conference Series 379 (2012) 012034. DOI: https://doi.org/10.1088/1742-6596/379/1/012034

[17] M.A. Wahid, A.N. Siddiquee, Z.A. Khan, Aluminum alloys in marine construction: characteristics, application, and problems from a fabrication viewpoint, Marine Systems and Ocean Technology 15 (2020) 70-80. DOI: https://doi.org/10.1007/s40868-019-00069-w

[18] S. Kumar, A.K. Srivastava, R.K. Singh, S.P. Dwivedi, Experimental study on hardness and fatigue behavior in joining of AA5083 and AA6063 by friction stir welding, Materials Today: Proceedings 25/4 (2020) 646-648. DOI: https://doi.org/10.1016/j.matpr.2019.07.535

[19] R. Koganti, A. Elliott, M. Zaluzec, A. Caliskan, A. Joaquin, Influence of Heat Treatment on Gas Metal Arc Welded Aluminum 6063 Alloy for Automotive Aluminum Spaceframe Architectures, Proceedings of the ASME 2008 International Mechanical Engineering Congress and Exposition. Volume 15: Processing and Engineering Applications of Novel Materials, Boston, Massachusetts, USA, 2008, 63-68. DOI: https://doi.org/10.1115/IMECE2008-68495

[20] B. Çevik, M. Koç, The effects of welding speed on the microstructure and mechanical properties of marine-grade aluminium (AA5754) alloy joined using MIG welding, Kovove Materialy/Metallic Materials 57/5 (2019) 307-316. DOI: https://doi.org/10.4149/km_2019_5_307

[21] J.A. Vargas, J.E. Torres, J.A. Pacheco, R.J. Hernandez, Analysis of heat input effect on the mechanical properties of Al-6061-T6 alloy weld joints, Materials and Design (1980-2015) 52 (2013) 556-564. DOI: https://doi.org/10.1016/j.matdes.2013.05.081

[22] R. Ahmad, M.A. Bakar, Effect of a post-weld heat treatment on the mechanical and microstructure properties of AA6061 joints welded by the gas metal arc welding cold metal transfer method, Materials and Design 32/10 (2011) 5120-5126. DOI: https://doi.org/10.1016/j.matdes.2011.06.007

[23] A.K. Lakshminarayanan, V. Balasubramanian, K. Elangovan, Effect of welding processes on tensile properties of AA6061 aluminium alloy joints, International Journal of Advanced Manufacturing Technology 40 (2009) 286-296. DOI: https://doi.org/10.1007/s00170-007-1325-0

[24] J. Qin, H. Nagaumi, C. Yu, F. Liu, Y. Li, L. Wang, Coarsening behavior of Mg_2Si precipitates during post homogenization cooling process in Al-Mg-Si alloy, Journal of Alloys and Compounds 902 (2022) 162851. DOI: https://doi.org/10.1016/j.jallcom.2021.162851

[25] S.M. Ashrafizadeh, A.R. Eivani, H.R. Jafarian, J. Zhou, Improvement of mechanical properties of AA6063 aluminum alloy after equal channel angular pressing by applying a two-stage solution treatment, Materials Science and Engineering A 687 (2017) 54-62. DOI: https://doi.org/10.1016/j.msea.2017.01.024

[26] H. Feng, Y. Chen, H. Yang, P. Yang, J. Zhang, B. Shu, Effects of Aging Treatment on the Mechanical Properties and Corrosion Resistance of an Al-Cu-Mg-Li Alloy, Materials Today: Communications 32 (2023) 105487. DOI: https://doi.org/10.1016/j.mtcomm.2023.105487

[27] S. Doddapaneni, S. Sharma, G.M.C. Shankar, M. Shettar, A. Hegde, Effect of precipitation hardening treatment on hardness and tensile behaviour of stir cast LM4 hybrid composites through TEM and fractography analysis, Journal of Materials Research and Technology 23 (2023) 1584-1598. DOI: https://doi.org/10.1016/j.jmrt.2023.01.127

[28] M. Thornton, L. Han, M. Shergold, Progress in NDT of resistance spot welding of aluminium using ultrasonic C-scan, NDT and E International 48 (2012) 30-38. DOI: https://doi.org/10.1016/j.ndteint.2012.02.005

[29] L. Yenumula, R.V. Acharya, B.M. Lingade, A. Borgohain, N.K. Maheshwari, U. Kumar, P.T. Selvam, A. Dash, Radiographic evaluation of gas tungsten arc welded joints used in nuclear applications by X- and gamma-rays, NDT and E International 102 (2019) 144-152. DOI: https://doi.org/10.1016/j.ndteint.2018.11.017

[30] O. Zahran, H. Kasban, M. El-Kordy, F.E.A. El-Samie, Automatic weld defect identification from radiographic images, NDT and E International 57 (2013) 26-35. DOI: https://doi.org/10.1016/j.ndteint.2012.11.005

[31] Z. Li, C. Li, Y. Liu, L. Yu, Q. Guo, H. Li, Effect of heat treatment on microstructure and mechanical property of Al-10%Mg_2Si alloy, Journal of Alloys and Compounds 663 (2016) 16-19. DOI: https://doi.org/10.1016/j.jallcom.2015.12.128

[32] C. Chen, M. Gao, H. Mu, X. Zeng, Effect of kerf characteristics on weld porosity of laser cutting-welding of AA2219 aluminum alloy, Applied Surface Science 494 (2019) 1036-1043. DOI: https://doi.org/10.1016/j.apsusc.2019.07.259

[33] I. Habibi, Triyono, N. Muhayat, A Review on Aluminum Arc Welding and It's Problems, in: U. Sabino, F. Imaduddin, A. Prabowo (eds), Proceedings of the 6th International Conference and Exhibition on Sustainable Energy and Advanced Materials, Lecture Notes in Mechanical Engineering, Springer, Singapore, 819-826. DOI: https://doi.org/10.1007/978-981-15-4481-1_78

[34] R.D. Ardika, T. Triyono, N. Muhayat, Triyono, A review porosity in aluminum welding, Procedia Structural Integrity 33 (2021) 171-180. DOI: https://doi.org/10.1016/j.prostr.2021.10.021

[35] S. Li, P. Jiang, Y. Gao, M. Song, L. Shu, A penetration depth monitoring method for Al-Cu laser lap welding based on spectral signals, Journal of Materials Processing Technology 317 (2023) 117972. DOI: https://doi.org/10.1016/j.jmatprotec.2023.117972

[36] L.F. Wang, J. Sun, X.L. Yu, Y. Shi, X.G Zhu, LY. Cheng, H.H. Liang, B. Yan, L.J. Guo, Enhancement in mechanical properties of selectively laser-melted AlSi10Mg aluminum alloys by T6-like heat treatment, Materials Science and Engineering A 734 (2018) 299-310. DOI: https://doi.org/10.1016/j.msea.2018.07.103

[37] A. Bahrami, A. Miroux, J. Sietsma, Modeling of strain hardening in the aluminum alloy AA606, Metallurgical and Materials Transactions A 44 (2013) 2409-2417. DOI: https://doi.org/10.1007/s11661-012-1594-6

[38] R.P. Verma, K.N. Pandey, Y. Sharma, Effect of ER4043 and ER5356 filler wire on mechanical properties and microstructure of dissimilar aluminium alloys, 5083-O and 6061-T6 joint, welded by the metal inert gas welding, Proceedings of the Institution of Mechanical Engineers, Part B: Journal of Engineering Manufacture 229/6 (2015) 1021-1028. DOI: https://doi.org/10.1177/0954405414535771

[39] R.P. Verma, K.N. Pandey, Multi-response optimization of process parameters of GMA welding of dissimilar AA 6061-T6 and AA 5083-O aluminium alloy for optimal mechanical properties, Materials Today: Proceedings 46/20 (2021) 10204-10210. DOI: https://doi.org/10.1016/j.matpr.2020.11.375

[40] R.P. Verma, Study of mechanical properties of GMA welded dissimilar aluminium alloys of AA5083-O/AA6061-T6 at different welding torch directions, Materials Today: Proceedings 46/20 (2021) 10306-10309. DOI: https://doi.org/10.1016/j.matpr.2020.12.454

[41] Ø. Ryen, B. Holmedal, O. Nijs, E. Nes, E. Sjölander, H.-E. Ekström, Strengthening Mechanisms in Solid Solution Aluminum Alloys, Metallurgical and Materials Transactions A 37 (2006) 1999-2006. DOI: https://doi.org/10.1007/s11661-006-0142-7

[42] A. Hidayat, A. Junaidi, S. Mudiantoro, W. Winarto, Fracture toughness and microstructure of gas metal arc welded plates of aluminium alloy 5083 using different filler wires and heat inputs, IOP Conference Series: Materials Science and Engineering 924 (2020) 012017. DOI: https://doi.org/10.1088/1757-899X/924/1/012017

[43] N. Li, W. Mao, X. Geng, R. Zhang, B. Yan, Microstructure, segregation and fracture behavior of 6061 aluminum alloy samples formed by semi-solid or traditional high pressure die casting, Materials Today: Communications 31 (2022) 103418. DOI: https://doi.org/10.1016/j.mtcomm.2022.103418

[44] F. Zupanič, J. Klemenc, M. Steinacher, S. Glodež, Microstructure, mechanical properties and fatigue behaviour of a new high-strength aluminium alloy AA 6086, Journal of Alloys and Compounds 941 (2023) 168976.
DOI: https://doi.org/10.1016/j.jallcom.2023.168976

[45] L. Huang, C. Wu, X. Hua, S. Liu, Z. Jiang, F. Li, F. H. Wang, S. Shi, Effect of the welding direction on the microstructural characterization in fiber laser-GMAW hybrid welding of 5083 aluminum alloy, Journal of Manufacturing Processes 31 (2018) 514-522. DOI: https://doi.org/10.1016/j.jmapro.2017.12.010